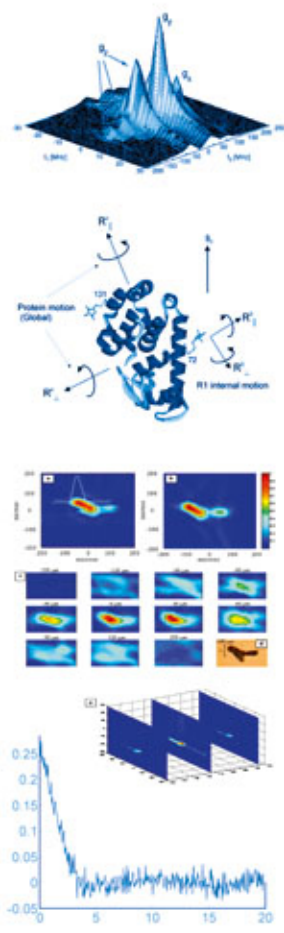
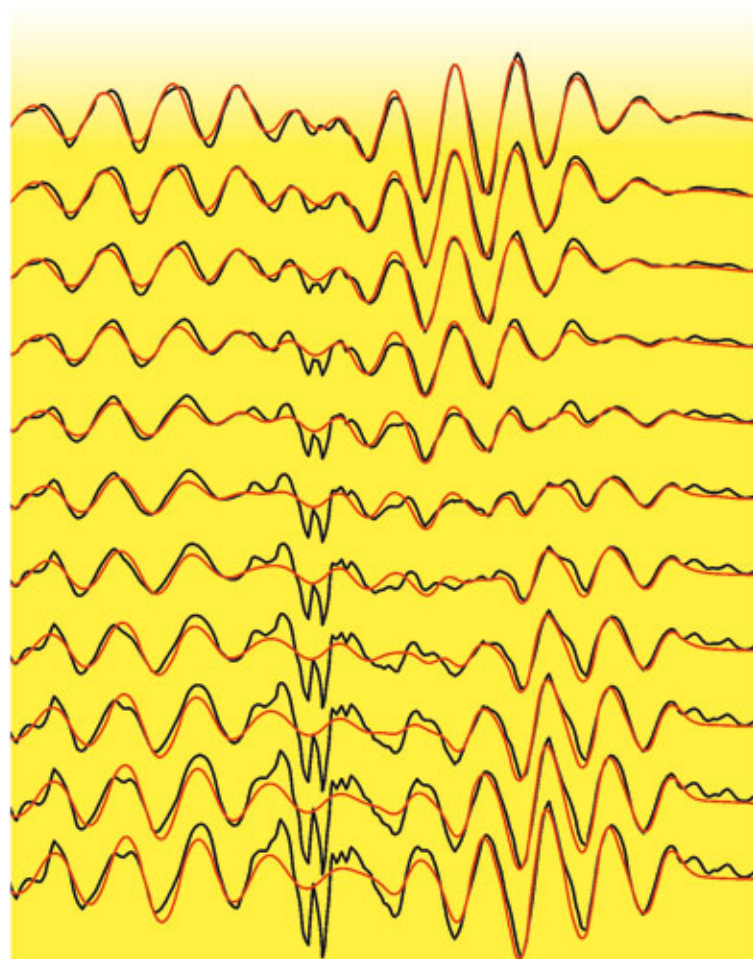


Multifrequency Electron Paramagnetic Resonance

Theory and Applications



Edited by
Sushil K. Misra

**Multifrequency Electron
Paramagnetic Resonance**

Details of the figures on the book cover

Left: The black traces are a set of model 1.6 GHz second-harmonic experimental EPR spectra corresponding to mixtures of 100–0% Cu(II)-imidazole and 0–100% Cu(II)-KTSM [3-ethoxy-2-oxobutyraldehyde-bis(N4-methylthiosemicarbazone) copper(II)], respectively, over the perpendicular region and the $m(I) = +1/2$ parallel line. The red traces are an automated fit to the model experimental spectra using simulations of the individual components as basis spectra. The simulations provided anisotropic copper and nitrogen hyperfine terms. The fits predicted the fraction of the major component to within 5% for each mixture. The feature at 580 G is a free radical contaminant in the Cu(II)-KTSM sample.

Right, from top to bottom: (i) SECSY: Two-Dimensional EPR spectrum of a spin labeled peptide: Gramicidin, in an aligned lipid membrane near room temperature taken at 95 GHz and showing its g-tensor resolution; (ii) An illustration of the model used to analyze multifrequency EPR spectra of spin-labeled proteins, in terms of internal and overall modes of motion. (iii) EPR micro-images of a LiPc crystal: (upper) 2D microimages; (middle) a series of 2D images for different Z-slice sections, lower right image is the optical image of the LiPc crystal; (bottom) a 3D stacking of the 2D images. (iv) The time domain Pulse-Dipolar EPR signal taken at 17 GHz from an RNA/DNA duplex corresponding to a distance between spin labels of 80 Å. The time evolution shown extends to 20 micro-secs.

Edited by Sushil K. Misra

Multifrequency Electron Paramagnetic Resonance

Theory and Applications



WILEY-
VCH

WILEY-VCH Verlag GmbH & Co. KGaA

The Editor**Prof. Dr. Sushil K. Misra**

Concordia University
Physics Department
1455 de Maisonneuve Blvd. West
Montreal, QC H3G 1M8
Canada

All books published by Wiley-VCH are carefully produced. Nevertheless, authors, editors, and publisher do not warrant the information contained in these books, including this book, to be free of errors. Readers are advised to keep in mind that statements, data, illustrations, procedural details or other items may inadvertently be inaccurate.

Library of Congress Card No.: applied for

British Library Cataloguing-in-Publication Data

A catalogue record for this book is available from the British Library.

**Bibliographic information published by the
Deutsche Nationalbibliothek**

The Deutsche Nationalbibliothek lists this publication in the Deutsche Nationalbibliografie; detailed bibliographic data are available on the Internet at <http://dnb.d-nb.de>.

© 2011 Wiley-VCH Verlag & Co. KGaA,
Boschstr. 12, 69469 Weinheim, Germany

All rights reserved (including those of translation into other languages). No part of this book may be reproduced in any form – by photoprinting, microfilm, or any other means – nor transmitted or translated into a machine language without written permission from the publishers. Registered names, trademarks, etc. used in this book, even when not specifically marked as such, are not to be considered unprotected by law.

Cover Formgeber, Eppelheim

Typesetting Toppan Best-set Premedia Limited

Printing and Binding Strauss GmbH, Mörlenbach

Printed in the Federal Republic of Germany
Printed on acid-free paper

ISBN: 978-3-527-40779-8

ePDF ISBN: 978-3-527-63354-8

ePub ISBN: 978-3-527-63355-5

oBook ISBN: 978-3-527-63353-1

Contents

Preface XXIX

List of Contributors XXXI

| | | |
|----------|--|----------|
| 1 | Introduction | 1 |
| | <i>Sushil K. Misra</i> | |
| 1.1 | Introduction to EPR | 1 |
| 1.1.1 | Continuous-Wave EPR | 1 |
| 1.1.2 | Pulsed EPR | 2 |
| 1.1.3 | EPR Imaging | 2 |
| 1.2 | Historical Background of EPR | 2 |
| 1.2.1 | Literature Pertinent to the Early History of EPR | 3 |
| 1.3 | Typical X-Band, Low-, and High-Frequency Spectrometers | 3 |
| 1.3.1 | EPR Spectrometer Design | 3 |
| 1.3.2 | X-Band Spectrometer | 4 |
| 1.3.2.1 | Source of Microwave Radiation | 4 |
| 1.3.2.2 | Transmission of Microwaves | 6 |
| 1.3.2.3 | The Cavity (Resonator) System | 6 |
| 1.3.2.4 | Magnetic Field System | 7 |
| 1.3.2.5 | Modulation and Detection System | 8 |
| 1.3.3 | EPR Line Shapes and Determination of Signal Intensity | 9 |
| 1.3.4 | Low-Frequency Spectrometers | 9 |
| 1.3.5 | High-Frequency Spectrometers | 10 |
| 1.3.5.1 | Sources of Radiation | 10 |
| 1.3.5.2 | Transmission of Submillimeter Waves | 12 |
| 1.3.5.3 | Resonators and Sensitivity | 13 |
| 1.3.5.4 | Magnetic Field | 14 |
| 1.3.5.5 | Detectors | 14 |
| 1.3.6 | Pertinent Literature | 15 |
| 1.4 | Applications of EPR | 15 |
| 1.4.1 | Pertinent Literature | 20 |

| | | |
|----------|--|-----------|
| 1.5 | Scope of This Book | 20 |
| | Acknowledgments | 21 |
| | Further Reading | 21 |
| 2 | Multifrequency Aspects of EPR | 23 |
| | <i>Sushil K. Misra</i> | |
| 2.1 | Frequency Bands | 23 |
| 2.2 | X-Band EPR | 23 |
| 2.3 | EPR at Higher Frequencies (HF) | 24 |
| 2.3.1 | Advantages | 24 |
| 2.3.2 | Disadvantages | 32 |
| 2.4 | Low-Frequency EPR | 34 |
| 2.4.1 | Advantages | 34 |
| 2.4.2 | Disadvantages | 38 |
| 2.5 | Multifrequency EPR | 39 |
| 2.5.1 | Advantages of Using Multifrequency EPR | 39 |
| 2.5.2 | Limitations of Using Multifrequency EPR | 51 |
| 2.5.3 | Size of Resonant Cavity at Different Frequencies | 51 |
| 2.5.4 | Signal-to-Noise Ratios at Different Frequencies | 53 |
| 2.5.5 | Multifrequency Aspects of Using Home-Built versus Commercial Spectrometers | 53 |
| 2.5.6 | Multifrequency Aspects of Sample-Related Problems | 53 |
| | Acknowledgments | 53 |
| | Pertinent Literature | 53 |
| | References | 54 |
| 3 | Basic Theory of Electron Paramagnetic Resonance | 57 |
| | <i>Sushil K. Misra</i> | |
| 3.1 | Introduction | 57 |
| 3.2 | Crystal-Field Theory | 58 |
| 3.2.1 | Introduction to CFT | 58 |
| 3.2.2 | Free Atoms and Ions | 59 |
| 3.2.3 | The Crystal-Field Description of Transition Group Ions in Crystals | 62 |
| 3.2.3.1 | <i>p</i> -Orbitals | 63 |
| 3.2.3.2 | <i>d</i> -Orbitals | 63 |
| 3.2.4 | Crystal Field Potential | 65 |
| 3.2.5 | Point Charge Model | 67 |
| 3.2.5.1 | Potentials for Cubic and Lower Symmetry | 68 |
| 3.2.6 | Equivalent Operators and the Wigner–Eckart Theorem | 69 |
| 3.2.7 | Properties of <i>d</i> -Electrons in Crystal Fields | 71 |
| 3.2.7.1 | Ions with Several <i>d</i> -Electrons: Strong- and Weak-Field Cases | 71 |
| 3.2.7.2 | Energies and Wave-Functions for <i>d</i> -Electrons | 74 |
| 3.2.7.3 | Crystal-Field Parameters for <i>d</i> -Electrons | 75 |
| 3.2.7.4 | Crystal-Field Splittings for $3d^1$ and $3d^9$ Configurations | 77 |

| | | |
|---------|--|-----|
| 3.2.7.5 | The Ground State and its Relationship to EPR: Quenching of Orbital Angular Momentum and Calculation of g-Factors | 78 |
| 3.2.8 | The Rare-Earth Ions | 80 |
| 3.2.8.1 | Crystal Fields for Rare-Earth Ions: Dominant Spin–Orbit Coupling | 81 |
| 3.2.9 | Irreducible Representations for CF Energy Levels | 81 |
| 3.2.10 | Critique of Crystal-Field Theory | 82 |
| 3.2.11 | Kramers' Theorem | 82 |
| 3.3 | Superposition Model (SPM) | 83 |
| 3.4 | Molecular Orbital (MO) Approach | 85 |
| 3.4.1 | Linear Combination of Atomic Orbitals (LCAO) | 85 |
| 3.4.2 | Extended Hückel Molecular Orbital Theory (EHMO) | 88 |
| 3.4.3 | Ligand Field Theory: The Angular Overlap Model (AOM) | 88 |
| 3.5 | The Jahn–Teller (JT) Effect | 92 |
| 3.5.1 | Theory of the JT Effect | 95 |
| 3.5.1.1 | General Theory of the JT Effect | 96 |
| 3.5.2 | Perturbation within the Vibronic Ground State | 98 |
| 3.5.3 | Three-State Model | 100 |
| 3.5.4 | Transition from Dynamic to Static JT Effect | 101 |
| 3.6 | The Spin Hamiltonian | 102 |
| 3.6.1 | The Abragam and Pryce Spin Hamiltonian for the Iron Group | 102 |
| 3.6.1.1 | Incorporation of Covalency | 105 |
| 3.6.2 | Zero-Field Splitting (ZFS) | 105 |
| 3.6.2.1 | Cubic Zero-Field Splitting ($S > 3/2$) | 106 |
| 3.6.3 | The Phenomenological Spin Hamiltonian | 106 |
| 3.6.3.1 | Triclinic Symmetry | 107 |
| 3.6.3.2 | Monoclinic Symmetry (C_{2h} , C_2 , C_{2s}) | 108 |
| 3.6.3.3 | Orthorhombic Symmetry (D_{2h} , D_2 , D_{2v}) | 108 |
| 3.6.3.4 | Tetragonal (D_{4h} , D_4 , C_{4v} , D_{2d} , C_{4h} , S_4 , and C_4) | 108 |
| 3.6.3.5 | Cubic (O_h , O , T_d , T_h , and T) and Spherical Symmetry | 108 |
| 3.6.3.6 | Additional Spin-Hamiltonian Terms with Higher Powers of Components of S | 108 |
| 3.6.4 | The Generalized Spin Hamiltonian | 110 |
| 3.6.5 | The Effective Spin Hamiltonian for EPR | 110 |
| 3.7 | Concluding Remarks | 111 |
| | Acknowledgments | 111 |
| | Pertinent Literature | 111 |
| | References | 111 |

Part One Experimental 115

| | | |
|-----|------------------------|-----|
| 4 | Spectrometers | 117 |
| 4.1 | Zero-Field EPR | 117 |
| | <i>Sushil K. Misra</i> | |

| | | |
|----------|---|-----|
| 4.1.1 | Introduction | 117 |
| 4.1.2 | Preliminary Theory of ZFR | 118 |
| 4.1.3 | The ZFR Spectrometer | 119 |
| 4.1.3.1 | Examples of ZFR Spectra | 119 |
| 4.1.4 | Advantages of Using Resonant Systems | 121 |
| 4.1.5 | Examples of ZFR | 121 |
| 4.1.5.1 | The Case of the Mn ²⁺ Ion | 122 |
| 4.1.6 | Concluding Remarks | 125 |
| | Pertinent Literature | 126 |
| | References | 128 |
| 4.2 | Low-Frequency CW-EPR Spectrometers: 10 MHz to 100 GHz | 128 |
| | <i>Harvey A. Buckmaster</i> | |
| 4.2.1 | Introduction | 128 |
| 4.2.2 | CW-EPR Spectrometer Configurations | 132 |
| 4.2.3 | Theoretical Sensitivity | 146 |
| 4.2.4 | EPR Lineshapes and Modulation Broadening | 148 |
| 4.2.5 | Microwave Power Sources | 149 |
| 4.2.6 | Reflex Klystrons | 151 |
| 4.2.7 | Solid-State Devices | 151 |
| 4.2.8 | Frequency Synthesizers | 153 |
| 4.2.9 | Microwave CW-EPR Sample Cavity Designs | 153 |
| 4.2.10 | Transmission Cavities | 156 |
| 4.2.11 | Reflection Cavities | 157 |
| 4.2.12 | Re-Entrant Cavities | 159 |
| 4.2.13 | Loop-Gap Cavities | 160 |
| 4.2.14 | Other Resonant Structures | 163 |
| 4.2.15 | Microwave Detectors or Demodulators | 164 |
| 4.2.15.1 | Point Contact Diodes | 164 |
| 4.2.15.2 | Schottky Barrier Diodes | 165 |
| 4.2.15.3 | Backward Diodes | 165 |
| 4.2.15.4 | Bolometers | 165 |
| 4.2.16 | Electromagnets | 166 |
| 4.2.17 | Zero-Field CW-EPR | 167 |
| 4.2.18 | Support Instrumentation | 168 |
| 4.2.19 | Concluding Remarks | 168 |
| 4.2.20 | Pertinent Literature | 169 |
| | References | 169 |
| | Appendix 4.2.I | 171 |
| | Appendix 4.2.II | 173 |
| | Appendix 4.2.III | 174 |
| 4.3 | High-Frequency EPR Spectrometers | 175 |
| | <i>Edward Reijerse</i> | |
| 4.3.1 | Introduction | 175 |
| 4.3.2 | High-Frequency EPR Spectrometer Configurations | 176 |
| 4.3.3 | Sensitivity Considerations | 182 |

| | | |
|----------|--|-----|
| 4.3.3.1 | Cavity and Sample Holder | 183 |
| 4.3.3.2 | Reflection Cavity with Square-Law Detector | 184 |
| 4.3.3.3 | Reflection Cavity with Linear Detector | 184 |
| 4.3.3.4 | Spectrometer Bridge and Detector | 185 |
| 4.3.4 | Conclusions and Future Perspectives | 188 |
| | Pertinent Literature | 188 |
| | References | 188 |
| 4.4 | Pulsed Techniques in EPR | 190 |
| | <i>Sankaran Subramanian and Murali C. Krishna</i> | |
| 4.4.1 | Introduction | 190 |
| 4.4.2 | Components of a Pulsed EPR Spectrometer | 193 |
| 4.4.2.1 | K _a -Band (26.5–40 GHz) Pulsed EPR Spectrometer | 194 |
| 4.4.2.2 | Radiofrequency Pulsed EPR Spectrometers Operating at 300, 500, and 750 MHz | 197 |
| 4.4.3 | Resonators | 199 |
| 4.4.4 | Pulsed Excitation and Relaxation | 202 |
| 4.4.5 | Fourier Transform in Magnetic Resonance | 202 |
| 4.4.6 | Simple Pulsed EPR Experiments | 203 |
| 4.4.6.1 | Inversion Recovery and Hahn Echo Pulse Sequences, T ₁ and T ₂ | 204 |
| 4.4.7 | Pulsed ENDOR, ESEEM, and HYSCORE | 208 |
| 4.4.7.1 | Nuclear Modulation Effects Leading to ENDOR and ESEEM | 209 |
| 4.4.7.2 | Mims and Davis Pulsed ENDOR Sequences | 211 |
| 4.4.8 | Electron Spin Echo Envelope Modulation (ESEEM) and Hyperfine Sublevel Correlation Spectroscopy (HYSCORE) | 214 |
| 4.4.9 | Electron–Electron Double Resonance (ELDOR), Double Electron–Electron Resonance (DEER), or Pulsed ELDOR (PELDOR) | 218 |
| 4.4.10 | Double-Quantum EPR | 220 |
| 4.4.11 | Concluding Remarks | 222 |
| | Pertinent Literature | 224 |
| | References | 225 |
| 5 | Multifrequency EPR: Experimental Considerations | 229 |
| 5.1 | Multiarm EPR Spectroscopy at Multiple Microwave Frequencies: Multiquantum (MQ) EPR, MQ-ELDOR, Saturation Recovery (SR) EPR, and SR-ELDOR | 229 |
| | <i>James S. Hyde, Robert A. Strangeway, and Theodore G. Camenisch</i> | |
| 5.1.1 | Introduction | 229 |
| 5.1.2 | Review of Frequency-Translation Techniques | 231 |
| 5.1.3 | Review of Multiarm Bridges | 233 |
| 5.1.4 | Multiarm Bridges at Higher Millimeter-Wave Frequencies | 236 |
| 5.1.5 | Resonator Considerations for Multiarm Experiments | 238 |
| 5.1.6 | Reference Arm and Receiver Design Considerations for Multiarm Experiments | 239 |
| 5.1.7 | Discussion | 241 |
| | Pertinent Literature | 243 |

| | | |
|---------|---|-----|
| | Acknowledgments | 243 |
| | References | 243 |
| 5.2 | Resonators for Multifrequency EPR of Spin Labels | 244 |
| | <i>James S. Hyde, Jason W. Sidabras, Richard R. Mett</i> | |
| 5.2.1 | Introduction | 244 |
| 5.2.2 | Methods | 247 |
| 5.2.2.1 | Computer-Based Simulations | 247 |
| 5.2.2.2 | Fabrication and Testing | 251 |
| 5.2.3 | Aqueous Samples | 252 |
| 5.2.3.1 | The Complex Dielectric Constant as a Function of Frequency and Temperature | 252 |
| 5.2.3.2 | Dielectric Loss Types and Parallel and Perpendicular E-Field Geometries | 253 |
| 5.2.3.3 | Results in Commercial Resonators at X-Band Using Extruded Sample Tubes | 255 |
| 5.2.3.4 | Multichannel Design | 256 |
| 5.2.4 | Uniform Field Cavities and Loop-Gap Resonators | 258 |
| 5.2.4.1 | Intrinsic Uniformity | 258 |
| 5.2.4.2 | Uniform Field Cavities | 258 |
| 5.2.4.3 | Uniformity in Two Dimensions | 258 |
| 5.2.4.4 | Loop-Gap Resonators | 259 |
| 5.2.5 | Coupling | 261 |
| 5.2.5.1 | Coupling at Low Frequencies | 262 |
| 5.2.5.2 | Coupling at High Frequencies | 262 |
| 5.2.6 | Field Modulation Penetration | 263 |
| 5.2.7 | Sample Access Stacks | 265 |
| 5.2.8 | Conclusions | 268 |
| | Pertinent Literature | 269 |
| | Acknowledgments | 269 |
| | References | 269 |
| 5.3 | Multifrequency EPR Sensitivity | 270 |
| | <i>George A. Rinard, Richard W. Quine, Sandra S. Eaton, and Gareth R. Eaton</i> | |
| 5.3.1 | Introduction | 270 |
| 5.3.1.1 | Nomenclature | 271 |
| 5.3.2 | Frequency Dependence of Sensitivity for an Ideal Spectrometer, at the Thermal Noise Limit | 272 |
| 5.3.2.1 | General Expression for SNR | 272 |
| 5.3.2.2 | Explanation of Table 5.3.2 | 275 |
| 5.3.2.3 | On Beyond the Predictions of Table 5.3.2 | 276 |
| 5.3.2.4 | Dependence of SNR on <i>g</i> -Anisotropy | 277 |
| 5.3.2.5 | Source Noise | 277 |
| 5.3.3 | Experimental Validation of Predicted Dependence of Sensitivity on Frequency | 279 |
| 5.3.3.1 | CW Spectrometers at Frequencies <10 GHz | 279 |

| | | |
|---------|---|-----|
| 5.3.3.2 | Pulsed EPR Spectrometers in the Frequency Range 250 MHz to 9.5 GHz | 279 |
| 5.3.3.3 | Summary of Experimental Validation of SNR of CW and Pulsed Spectrometers at Frequencies of <10 GHz | 280 |
| 5.3.4 | Reference Samples for SNR: Weak Pitch | 281 |
| 5.3.5 | Performance of High-Frequency (≥ 94 GHz)/High-Field EPR Spectrometers | 282 |
| 5.3.5.1 | CW Spectrometers | 282 |
| 5.3.5.2 | Pulsed EPR Spectrometers | 282 |
| 5.3.6 | Reported Sensitivities of CW and Pulsed Spectrometers at Various Frequencies | 285 |
| 5.3.6.1 | Further Details on CW EPR Sensitivity | 286 |
| 5.3.7 | Sensitivity Aspects Beyond the Minimum Detectable Number of Spins: Frequency Dependence of Pulse and CW Measurements Related to Distances Between Spins | 288 |
| 5.3.7.1 | Electron–Electron Coupling | 288 |
| 5.3.7.2 | Electron–Nuclear Coupling | 289 |
| 5.3.7.3 | Summary | 289 |
| 5.3.8 | Limitations of Sensitivity Considerations | 289 |
| 5.3.8.1 | CW Spectrometers | 289 |
| 5.3.8.2 | Resonators | 290 |
| 5.3.8.3 | Samples | 190 |
| 5.3.8.4 | Pulse Spectrometers | 290 |
| 5.3.9 | Conclusions | 290 |
| | Acknowledgments | 291 |
| | Pertinent Literature | 291 |
| | References | 292 |

Part Two Theoretical 295

| | | |
|----------|--|-----|
| 6 | First Principles Approach to Spin-Hamiltonian Parameters | 297 |
| | <i>Frank Neese</i> | |
| 6.1 | Introduction | 297 |
| 6.2 | The Spin Hamiltonian | 298 |
| 6.3 | Electronic Structure Theory of Spin-Hamiltonian Parameters | 300 |
| 6.3.1 | Electronic Structure Methods | 300 |
| 6.3.2 | Additional Terms in the Hamiltonian | 305 |
| 6.3.3 | Sum-Over States Theory of Spin Hamiltonian Parameters | 307 |
| 6.3.4 | Linear Response Theory | 310 |
| 6.3.5 | Expression for Spin-Hamiltonian Parameters for Self-Consistent Field Methods | 314 |
| 6.3.6 | Practical Aspects | 320 |
| 6.3.6.1 | Choice of Molecular Model | 320 |
| 6.3.6.2 | Choice of Geometry | 320 |

| | | |
|----------|--|------------|
| 6.3.6.3 | Choice of Theoretical Method | 321 |
| 6.3.6.4 | Choice of Basis Set | 322 |
| 6.3.6.5 | Summary and Recommendations | 323 |
| 6.4 | Concluding Remarks | 323 |
| | Acknowledgments | 324 |
| | Pertinent Literature | 325 |
| | References | 325 |
| 7 | Spin Hamiltonians and Site Symmetries for Transition Ions | 327 |
| | <i>Sushil K. Misra</i> | |
| 7.1 | Introduction | 327 |
| 7.2 | Spin Hamiltonians | 328 |
| 7.3 | Spin-Hamiltonian Terms for Various Site Symmetries | 332 |
| 7.4 | Transition Ions | 333 |
| 7.4.1 | Introduction to Transition-Metal Ions | 333 |
| 7.4.2 | First-Transition Series Ions ($3d^n$, Iron-Group Ions) | 333 |
| 7.4.3 | Second and Third Transition Series (The 4d, Palladium and 5d, Platinum Groups) | 345 |
| 7.4.4 | Rare-Earth Ions | 347 |
| 7.4.4.1 | Odd Number of 4f Electrons | 350 |
| 7.4.4.2 | Even Number of 4f Electrons | 350 |
| 7.4.5 | Actinide Ions ($5f^n$) | 354 |
| 7.4.5.1 | 5f ¹ Configuration | 354 |
| 7.4.5.2 | 5f ² Configuration | 356 |
| 7.4.5.3 | 5f ³ Configuration ($^4I_{9/2}$; U ³⁺ , Np ⁴⁺) | 357 |
| 7.4.6 | S-State Ions | 358 |
| 7.4.6.1 | Introduction | 358 |
| 7.4.6.2 | Spin Hamiltonian | 358 |
| 7.4.6.3 | Theoretical Considerations | 359 |
| 7.5 | Concluding Remarks | 363 |
| | Acknowledgments | 363 |
| | Pertinent Literature | 363 |
| | References | 363 |
| | Appendix 7.I Spin Operators and Their Matrix Elements | 365 |
| | Appendix 7.II Descent of Symmetry | 381 |
| | Appendix 7.III Site Symmetries of Host Crystals | 382 |
| 8 | Evaluation of Spin-Hamiltonian Parameters from Multifrequency EPR Data | 385 |
| | <i>Sushil K. Misra</i> | |
| 8.1 | Introduction | 385 |
| 8.2 | Perturbation Approach | 386 |
| 8.2.1 | Spin Hamiltonian | 387 |
| 8.2.1.1 | $S = 7/2$ | 390 |
| 8.2.1.2 | $S = 5/2$ (Fe ³⁺) | 391 |

| | | |
|---------|--|-----|
| 8.3 | Brute-Force Methods to Evaluate SHP | 394 |
| 8.3.1 | Variation of One Parameter at a Time | 394 |
| 8.3.2 | Variation of Parameters in Subgroups | 395 |
| 8.4 | Least-Squares Fitting (LSF) Method | 395 |
| 8.4.1 | Introduction | 395 |
| 8.4.2 | Details of the LSF Method as Applied to EPR | 397 |
| 8.4.3 | Determination of Parameter Errors | 399 |
| 8.4.4 | General Strategies for Achieving Convergence | 400 |
| 8.4.4.1 | Use of Interpolated Fields: Calculation of Resonant Field Values | 400 |
| 8.4.4.2 | Use of Interpolated Frequencies | 401 |
| 8.4.4.3 | Use of Binary Chop (Misra, 1976) | 401 |
| 8.5 | Other Applications of the LSF Method | 401 |
| 8.5.1 | Electron–Nuclear Spin-Coupled Systems (Misra, 1983) | 402 |
| 8.5.1.1 | Estimation of Initial Values of FS SHPs | 402 |
| 8.5.1.2 | Estimation of HFS Parameters | 403 |
| 8.5.1.3 | Identification of Energy Levels Participating in Resonance | 403 |
| 8.5.1.4 | Construction of the SH Matrix for ENSC Systems | 403 |
| 8.5.1.5 | Absolute Signs of SH Parameters | 404 |
| 8.5.2 | Fitting of ENDOR Data | 404 |
| 8.5.3 | Calculation and Fitting of Line Intensities to SHP | 404 |
| 8.5.3.1 | The Intensity Operator | 405 |
| 8.5.3.2 | Fitting of Line Intensities and Line Positions to SHP | 405 |
| 8.5.3.3 | Normalized Intensity and its Derivatives | 406 |
| 8.5.3.4 | Limits of Applicability of the Method | 408 |
| 8.6 | Concluding Remarks | 408 |
| | Acknowledgments | 410 |
| | Pertinent Literature | 410 |
| | References | 410 |
| | Appendix 8.I Historical Review | 411 |

| | | |
|----------|--|-----|
| 9 | Simulation of EPR Spectra | 417 |
| | <i>Sushil K. Misra</i> | |
| 9.1 | Introduction | 417 |
| 9.2 | Simulation of Single-Crystal Spectrum | 417 |
| 9.2.1 | Transition Probability | 418 |
| 9.2.2 | Single-Crystal Lineshape Function $F(B_{ri}, B_k)$ | 420 |
| 9.3 | Simulation of a Polycrystalline Spectrum | 421 |
| 9.3.1 | Angular Variation of EPR Spectra: Homotopy Technique | 421 |
| 9.3.1.1 | Computation of the Initial Resonant Fields $B_r(\theta, \phi)$ | 422 |
| 9.3.1.2 | Computation of the First and Second Derivatives of χ^2 with Respect to B | 422 |
| 9.3.1.3 | Problems Encountered in the Application of Homotopy Method, and their Solutions | 423 |
| 9.3.2 | Lineshapes | 424 |
| 9.3.3 | Transition Probabilities | 424 |

| | | |
|-----------|--|------------|
| 9.3.4 | Resonance Eigenpairs | 424 |
| 9.3.5 | Integrals | 425 |
| 9.3.6 | (θ_j, ϕ_j) Grid | 426 |
| 9.3.7 | Steps Required in Simulation of Powder Spectrum | 426 |
| 9.3.7.1 | Calculation of First-Derivative EPR Spectrum | 428 |
| 9.3.8 | Illustrative Example | 429 |
| 9.3.9 | Additional remarks | 429 |
| 9.4 | Evaluation of Spin-Hamiltonian (SH) Parameters and the Linewidth from a Polycrystalline EPR Spectrum | 429 |
| 9.4.1 | Estimation of Spin-Hamiltonian Parameters from a Polycrystalline Spectrum | 430 |
| 9.4.1.1 | Estimation of D and E Parameters for the Mn^{2+} Ion from Forbidden Hyperfine Doublet Separations in Polycrystalline Samples in the Central Sextet | 430 |
| 9.4.1.2 | Rigorous Evaluation of SH Parameters from a Polycrystalline Spectrum by Using Matrix Diagonalization and Least-Squares Fitting | 432 |
| 9.4.1.3 | Evaluation of SH Parameters and Linewidths for the Case of Two Magnetically Inequivalent Species | 436 |
| 9.4.1.4 | Illustrative Example | 436 |
| 9.4.1.5 | General Remarks | 437 |
| 9.5 | Simulation of EPR Spectra in Disordered Materials: Application to Glassy Materials | 437 |
| 9.5.1 | Introduction | 437 |
| 9.5.2 | Computer Simulation of EPR Spectra in Glasses | 437 |
| 9.5.3 | Computer-Simulated Spectra and Comparison with Experiment | 440 |
| 9.5.4 | Shape of EPR Spectra in Glasses: Effect of SH Parameters | 442 |
| 9.5.4.1 | Distribution of the Fine-Structure Parameters D and E | 442 |
| 9.5.4.2 | Sharp Features in Spectra | 447 |
| 9.5.4.3 | Broad Resonances in Spectra | 448 |
| 9.6 | Simulation of EPR Spectra in Disordered Random Network Materials | 448 |
| 9.6.1 | Introduction | 448 |
| 9.6.2 | CW-EPR Spectrum for Random Distribution of SH Parameters at Various Sites in Glasses | 449 |
| 9.6.2.1 | Calculation of Eigenvectors $ i'\rangle$ and $ i''\rangle$ Required in Equation 9.57 | 450 |
| 9.6.3 | Limitations of the Original Implementation and its Assumptions | 450 |
| | Acknowledgments | 451 |
| | Pertinent Literature | 451 |
| | References | 451 |
| | Appendix 9.I The Eigenfield Equation | 453 |
| 10 | Relaxation of Paramagnetic Spins | 455 |
| | <i>Sushil K. Misra</i> | |
| 10.1 | Introduction | 455 |

| | | |
|----------|--|-----|
| 10.2 | Equilibrium Magnetization of a Paramagnetic Spin System | 457 |
| 10.3 | Relaxation Phenomena: Spin–Lattice and Spin–Spin Relaxation Times | 458 |
| 10.3.1 | Bloch's Equations | 459 |
| 10.4 | Rotating Frame | 459 |
| 10.5 | Experimental Techniques to Measure Relaxation Times | 460 |
| 10.5.1 | CW-EPR Techniques (Bertini, Martini, and Luchinat, 1994) | 461 |
| 10.5.1.1 | CW Saturation | 461 |
| 10.5.2 | Longitudinally Detected Paramagnetic Resonance (LODEPR) to Measure Short Relaxation times (10^{-8} s) (Giordano et al., 1981) | 463 |
| 10.5.3 | Amplitude Modulation Technique to Measure Very Short Relaxation Times ($10^{-6} - 10^{-9}$ s) (Misra, 2005) | 463 |
| 10.5.4 | Pulsed EPR Techniques to Measure Relaxation Times | 463 |
| 10.5.5 | Long Pulse Saturation Recovery Using CW Detection (Huisjen and Hyde, 1974; Percival and Hyde, 1975; Eaton and Eaton, 2000) | 464 |
| 10.5.6 | Inversion Recovery (Eaton and Eaton, 2000) | 464 |
| 10.5.7 | Electron Spin Echo (ESE) Technique (Schweiger and Jeschke, 2001) | 464 |
| 10.5.8 | Long-Pulse Saturation with Spin-Echo Detection | 465 |
| 10.5.9 | Picket-Fence Excitation (Eaton and Eaton, 2000) | 465 |
| 10.5.10 | Echo Repetition Rate (Eaton and Eaton, 2000) | 465 |
| 10.5.11 | Three-Pulse-Stimulated Echo (Eaton and Eaton, 2000) | 466 |
| 10.5.12 | Longitudinally Detected Pulsed EPR (LODPEPR) (Schweiger, 1991; Schweiger and Ernst, 1988) | 466 |
| 10.5.13 | Other Pulse Techniques | 466 |
| 10.5.14 | Measurements of Relaxation Time by Line-Shape Analysis: Linewidth and Spin–Spin Relaxation Time | 466 |
| 10.5.15 | Temperature-Dependent Contribution to EPR Linewidth (Poole and Farach, 1971) | 467 |
| 10.5.16 | Non-EPR Techniques to Measure Relaxation Times | 467 |
| 10.6 | Relaxation Mechanisms | 468 |
| 10.6.1 | Spin-Lattice Relaxation in Diluted Ionic Solids in the Crystalline State | 468 |
| 10.6.1.1 | General Background | 468 |
| 10.6.1.2 | The Direct Process | 469 |
| 10.6.1.3 | The Orbach Process (Orbach and Stapleton, 1972; Orbach, 1961a, 1961c) | 471 |
| 10.6.1.4 | Two-Phonon Raman Process | 471 |
| 10.6.1.5 | SLR due to Exchange Interaction | 473 |
| 10.6.2 | Relaxation in Amorphous Systems | 474 |
| 10.6.2.1 | Relaxation via TLS Centers | 475 |
| 10.6.2.2 | SLR Effected by Electron–Nuclear Dipolar Coupling to a TLS Center | 477 |
| 10.6.2.3 | SLR due to Fermi-Contact Hyperfine Interaction with a TLS Center | 478 |

| | | |
|-----------|--|------------|
| 10.6.2.4 | Temperature Dependence of Relaxation Rate in Amorphous Materials due to Exchange Interaction | 478 |
| 10.6.2.5 | Relaxation for the Case of Strong Cross-Relaxation and Weak Spin-Lattice Relaxation of Single Ions in Amorphous Materials (Al'tshuler, 1956) | 478 |
| 10.6.3 | Relaxation in Diluted Liquid Solutions | 479 |
| 10.6.4 | Effect of Intramolecular Dynamics of Molecular Species on Relaxation | 483 |
| 10.6.4.1 | Dephasing by Methyl Groups in Solvent or Surroundings | 483 |
| 10.6.4.2 | Shape of the Echo-Decay Curve | 484 |
| 10.6.4.3 | Averaging of Electron-Nuclear Couplings due to Rotation of Methyl Groups | 484 |
| 10.6.4.4 | Effect of a Rapidly Relaxing Partner on Electron–Electron Spin–Spin Coupling | 484 |
| 10.6.4.5 | Librational Motion | 484 |
| 10.6.4.6 | Molecular Tumbling | 484 |
| 10.6.4.7 | Biomolecules | 485 |
| 10.6.4.8 | Macromolecules | 485 |
| 10.6.5 | Relaxation among Different Paramagnetic Centers in Concentrated Solution | 485 |
| 10.6.6 | Spin-Fracton Relaxation | 485 |
| 10.6.6.1 | One-Fracton Emission | 486 |
| 10.6.6.2 | Two-Fracton Inelastic Scattering (Localized Electronic State) (Alexander, Entin-Wohlman, and Orbach, 1985a) | 487 |
| 10.6.7 | Frequency/Field Dependence of Paramagnetic Relaxation | 489 |
| | Pertinent literature | 490 |
| | Acknowledgments | 491 |
| | References | 491 |
| | Appendix 10.I Early History of Paramagnetic Spin-Lattice Relaxation | 494 |
| 11 | Molecular Motions | 497 |
| | <i>Sushil K. Misra and Jack H. Freed</i> | |
| 11.1 | Introduction | 497 |
| 11.2 | Historical Background | 498 |
| 11.3 | High-Field Multifrequency CW-EPR Experiments to Unravel Molecular Motion | 500 |
| 11.3.1 | Determination of the Axes of Motion from High-Field, High-Frequency (HFHF) EPR Spectra: Orientational Resolution | 503 |
| 11.3.2 | Observation of Motion as a Function of Frequency | 504 |
| 11.3.3 | Virtues of Multifrequency EPR in Studying Molecular Motion | 504 |
| 11.3.4 | Stochastic Liouville Equation (SLE) to Describe Slow-Motional EPR Spectra | 505 |
| 11.3.4.1 | Calculation of Slow-Motion Spectrum | 506 |
| 11.3.4.2 | MOMD and SRLS Models | 511 |

| | | |
|-----------|---|------------|
| 11.4 | Pulsed EPR Study of Molecular Motion | 514 |
| 11.4.1 | T_2 -Type Field-Swept 2D ESE | 515 |
| 11.4.2 | Magnetization Transfer by Field-Swept 2-D-ESE | 515 |
| 11.4.3 | Stepped-Field Spin-Echo ELDOR | 517 |
| 11.4.4 | 2-D Fourier Transform EPR | 517 |
| 11.4.4.1 | Lineshapes of the Auto and Cross-Peaks: Homogeneous (HB) and Inhomogeneous Broadening (IB) | 518 |
| 11.4.5 | MOMD and SRLS Models and 2-D-ELDOR | 520 |
| 11.4.6 | Extension of 2-D-ELDOR to Higher Frequencies | 522 |
| 11.5 | Simulation of Multifrequency EPR Spectra Using More Atomistic Detail Including Molecular Dynamics and Stochastic Trajectories | 522 |
| 11.5.1 | Augmented SLE | 522 |
| 11.5.2 | MD Simulations Using Trajectories | 524 |
| 11.5.3 | Use of Dynamic Trajectories to Simulate Multifrequency EPR Spectra | 525 |
| 11.5.4 | Numerical Integrators | 526 |
| 11.5.4.1 | Integration of the Quantal Spin Dynamics | 526 |
| 11.5.4.2 | Generation of Stochastic Trajectories for Rotational Diffusion | 531 |
| 11.5.4.3 | Testing the Integrators: Generation of Trajectories for Typical Stochastic Models of Spin-Label Dynamics | 535 |
| 11.6 | Concluding Remarks | 541 |
| | Acknowledgments | 541 |
| | Pertinent Literature | 541 |
| | References | 542 |
| 12 | Distance Measurements: Continuous-Wave (CW)- and Pulsed Dipolar EPR | 545 |
| | <i>Sushil K. Misra and Jack H. Freed</i> | |
| 12.1 | Introduction | 545 |
| 12.2 | The Dipolar Interaction and Distance Measurements | 547 |
| 12.2.1 | Unlike Spins | 547 |
| 12.2.2 | Like Spins | 548 |
| 12.2.3 | Intermediate Case | 548 |
| 12.3 | CW EPR Method to Measure Distances | 548 |
| 12.4 | Pulsed Dipolar EPR Spectroscopy (PDS) | 549 |
| 12.5 | Double Electron–Electron Resonance (DEER) | 550 |
| 12.5.1 | Orientation-Selection Considerations in DEER | 552 |
| 12.5.2 | Three-Pulse DEER | 553 |
| 12.5.3 | Four-Pulse DEER | 555 |
| 12.5.4 | Merits and Limitations of DEER as Compared to CW-EPR and FRET | 557 |
| 12.6 | Six-Pulse DQC | 559 |
| 12.6.1 | Theoretical Background and Computation of Six-Pulse DQC Signal | 562 |
| 12.6.2 | Illustrative Examples | 566 |

| | | |
|-----------------|---|-----|
| 12.6.3 | Conclusions and Future Prospects of Six-Pulse DQC Echo Signal Simulation | 566 |
| 12.7 | Sensitivity Considerations: Multifrequency Aspects | 570 |
| 12.7.1 | Frequency Dependence of Sensitivity of PDS | 572 |
| 12.8 | Distance Distributions: Tikhonov Regularization | 573 |
| 12.9 | Additional Technical Aspects of DEER and DQC | 574 |
| 12.10 | Concluding Remarks | 576 |
| | Acknowledgments | 576 |
| | Pertinent Literature | 576 |
| | References | 576 |
| Appendix 12.I | Density-Matrix Derivation of Echo Signal for Three-Pulse DEER | 578 |
| Appendix 12.II | Density-Matrix Derivation of the Echo Signal for Four-Pulse DEER | 582 |
| Appendix 12.III | Spin Hamiltonian for Coupled Nitroxides Used in Six-Pulse DQC Calculation | 584 |
| Appendix 12.IV | Algorithm to Calculate Six-Pulse DQC Signal | 586 |
| Appendix 12.V | Approximate Analytic Expressions for 1-D DQC Signal | 587 |

Part Three Applications 589

| | | |
|-----------|--|-----|
| 13 | Determination of Large Zero-Field Splitting | 591 |
| | <i>Sushil K. Misra</i> | |
| 13.1 | Introduction | 591 |
| 13.2 | ZFS of Kramers and Non-Kramers Ions in Different Environments | 592 |
| 13.3 | Concluding Remarks | 596 |
| | Acknowledgments | 597 |
| | Pertinent Literature | 597 |
| | References | 597 |
| 14 | Determination of Non-Coincident Anisotropic \tilde{g}^2, \tilde{A}^2, \tilde{D}, and \tilde{P} Tensors: Low-Symmetry Considerations | 599 |
| | <i>Sushil K. Misra</i> | |
| 14.1 | Introduction | 599 |
| 14.2 | Spin Hamiltonian | 599 |
| 14.3 | Eigenvalues | 601 |
| 14.3.1 | Perturbation Approach | 601 |
| 14.3.1.1 | Complexities Associated with the Use of Second-Order-Perturbed Eigenvalues in the Application of Least-Squares Fitting (LSF) Procedure | 604 |
| 14.3.2 | Exact Matrix Diagonalization | 605 |
| 14.4 | Evaluation of SHPs by the LSF Technique | 606 |
| 14.4.1 | First-Order Perturbation | 606 |

| | | |
|-----------|--|------------|
| 14.4.2 | Second-Order Perturbation | 607 |
| 14.4.3 | Use of Special Coordinate Axes | 609 |
| 14.4.3.1 | “Allowed” Line Positions | 609 |
| 14.4.3.2 | “Forbidden” Line Positions | 611 |
| 14.4.4 | Use of Arbitrary Coordinate Axes | 612 |
| 14.4.5 | Simultaneous LSF Fitting of Both the “Allowed” and “Forbidden” Line Positions | 613 |
| 14.5 | Numerical Evaluation of the Derivatives Required in the LSF Procedure | 614 |
| 14.6 | General Remarks | 616 |
| | Acknowledgments | 618 |
| | Pertinent Literature | 618 |
| | References | 618 |
| 15 | Biological Systems | 619 |
| | <i>Boris Dzikovski</i> | |
| 15.1 | Introduction | 619 |
| 15.2 | VHF EPR as the <i>g</i> -Resolved EPR Spectroscopy | 620 |
| 15.2.1 | Spectral Resolution of <i>g</i> -Factor Differences | 620 |
| 15.2.2 | Precise Determination of the <i>g</i> -Tensor Principal Values | 621 |
| 15.2.3 | Resolution of <i>g</i> -Factors of Different Paramagnetic Centers | 622 |
| 15.3 | Effect of Polarity of the Environment on the <i>g</i> -Factor | 623 |
| 15.3.1 | Examples | 623 |
| 15.3.1.1 | Derivatives of 2,2,6,6-tetramethylpiperidine-1-oxyl (TEMPO) | 623 |
| 15.3.1.2 | Spin-Labeled Phospholipid Membranes: 1,2-Dipalmitoyl- <i>sn</i> -Glycero-3-Phosphocholine (DPPC) and 1-Palmitoyl-2-Oleoyl- <i>sn</i> -Glycero-3-Phosphocholine (POPC) | 625 |
| 15.3.1.3 | Bacteriorhodopsin (BR) | 625 |
| 15.3.1.4 | Azurin | 626 |
| 15.3.1.5 | Tyrosyl and Tryptophan Radicals | 626 |
| 15.3.1.6 | Flavin | 626 |
| 15.3.1.7 | Biliverdin Radical | 627 |
| 15.3.2 | Polarity Measurements Outside of Rigid Limit Conditions | 627 |
| 15.4 | Improvement in Orientational Resolution for Spin Labels | 628 |
| 15.5 | Simulation of EPR Spectra at Various Frequencies: Simple Limiting Cases | 630 |
| 15.6 | Macroscopically Aligned Phospholipid Membranes | 631 |
| 15.6.1 | A “Shunt” Fabry-Pérot Resonator. The study of DMPC and DMPS (1,2-dimyristoyl- <i>sn</i> -glycero-3-phospho-L-serine) Membranes with 3-doxy-5-(cholestane) (CSL) Spin Label | 632 |
| 15.6.2 | Microtome Technique on Isopotential Spin-Dry Ultracentrifugation (ISDU)-Aligned Membranes | 633 |
| 15.6.3 | Other Membrane-Alignment Techniques | 635 |
| 15.7 | Metalloproteins | 636 |
| 15.7.1 | Fe ³⁺ Systems | 638 |

| | | |
|-----------|--|------------|
| 15.7.2 | Mn ²⁺ Systems | 638 |
| 15.7.3 | Cu ²⁺ Systems | 639 |
| 15.8 | Concluding Remarks | 641 |
| | Acknowledgments | 642 |
| | Pertinent Literature | 642 |
| | References | 643 |
| 16 | Copper Coordination Environments | 647 |
| | <i>William E. Antholine, Brian Bennett, and Graeme R. Hanson</i> | |
| 16.1 | Introduction | 647 |
| 16.2 | Multifrequency EPR Toolkit | 649 |
| 16.2.1 | g-Value Resolution and Orientation Selection | 649 |
| 16.2.2 | Magnitude of the Microwave Frequency | 650 |
| 16.2.3 | State Mixing | 650 |
| 16.2.4 | Angular Anomalies | 652 |
| 16.2.5 | Distribution of Spin Hamiltonian Parameters | 653 |
| 16.2.6 | Numerical Differentiation and Fourier Filtering | 655 |
| 16.2.7 | High-Resolution EPR Techniques | 655 |
| 16.2.8 | Computer Simulation | 656 |
| 16.2.9 | Computational Chemistry | 658 |
| 16.3 | Multifrequency EPR Simulation of Square–Planar-Based Cu(II) | 660 |
| 16.3.1 | EPR of Square–Planar-Based Cu(II) | 660 |
| 16.3.2 | Multifrequency EPR of Square–Planar-Based Cu(II): S- and L-Band EPR | 660 |
| 16.3.3 | Multifrequency EPR of Square–Planar-Based Cu(II): Very Low-Frequency EPR | 661 |
| 16.3.4 | Multifrequency EPR of Square–Planar-Based Cu(II): Experimental Considerations for Low-Frequency EPR | 663 |
| 16.3.5 | Introduction to Multifrequency EPR Simulations of Square–Planar Cu(II) | 664 |
| 16.3.6 | Optimum Frequency Selection | 665 |
| 16.3.7 | Sensitivity Analysis | 668 |
| 16.3.8 | Global Fitting | 669 |
| 16.3.8.1 | Mo(V) Complexes | 671 |
| 16.3.8.2 | Low-Spin Co(II) Crossover Complexes | 673 |
| 16.3.8.3 | Future Developments | 675 |
| 16.3.9 | Heterogeneity | 675 |
| 16.4 | Copper-Coordination Environments: Multifrequency EPR of Three-Coordinate Copper and Mixed-Valence Dinuclear Copper [Cu(1.5 ⁺) ... Cu(1.5 ⁺)] | 677 |
| 16.4.1 | Introduction: Spectrum and Structure | 677 |
| 16.4.1.1 | X-Band EPR Spectrum for Mononuclear, Light Blue Cu ²⁺ | 677 |
| 16.4.1.2 | Peisach–Blumberg-Like Table (EPR Parameters Assembled by the Author) | 677 |
| 16.4.1.3 | Type 1 (Blue) Copper Centers, Three-Coordinate Cu | 678 |

| | | |
|-----------|---|------------|
| 16.4.2 | EPR for New Three-Coordinate Copper Complexes | 681 |
| 16.4.2.1 | Three-Coordinate CuL(SCPh ₃) and Copper(II) Phenolate Complexes | 681 |
| 16.4.2.2 | CuPPN, Three-Coordinate Copper Amido and Aminyl Complexes (More Like a Free Radical) | 681 |
| 16.4.2.3 | Simulation of Spectra for CuPPN (Quenched EPR Parameters Expected for a Radical) | 682 |
| 16.4.2.4 | EPR Parameters for CuPPN (Unpaired Electron Density Delocalized as Expected for a Radical) | 685 |
| 16.4.3 | Spectra for Mixed-Valence Dinuclear Copper Complexes | 686 |
| 16.4.3.1 | Nitrous Oxide Reductase, N ₂ OR (¹⁵ N Example) | 686 |
| 16.4.3.2 | Perturbation of the EPR Spectrum of Cu _A , H12OX | 689 |
| 16.4.3.3 | Cytochrome c Oxidase (CcO): Best Demonstration of the Use of Low-Frequency for Mixed-Valence Sites | 691 |
| 16.4.3.4 | Model Diamond Core Complexes, {Cu(LXL)} ₂ ⁺ | 695 |
| 16.4.3.5 | X-Band EPR Spectra of {Cu(PPP)} ₂ ⁺ , {Cu(PNP)} ₂ ⁺ , and {Cu(SNS)} ₂ ⁺ | 695 |
| 16.4.3.6 | Q-Band EPR Spectra of {Cu(PPP)} ₂ ⁺ , {Cu(PNP)} ₂ ⁺ , and {Cu(SNS)} ₂ ⁺ | 695 |
| 16.4.3.7 | S-Band Spectra of {Cu(PPP)} ₂ ⁺ , {Cu(PNP)} ₂ ⁺ , and {Cu(SNS)} ₂ ⁺ | 697 |
| 16.4.3.8 | EPR Parameters and Simulations for {Cu(SNS)} ₂ ⁺ | 697 |
| 16.4.3.9 | First-Harmonic S-Band Spectrum for {Cu(PPP)} ₂ ⁺ | 697 |
| 16.5 | Structural Characterization of Copper(II) Cyclic Peptide Complexes Employing Multifrequency EPR and Computational Chemistry | 699 |
| 16.5.1 | Copper(II) Complexes with Marine Cyclic Peptides | 701 |
| 16.5.2 | Copper(II) Complexes with Westiellamide and Synthetic Analogs | 707 |
| 16.6 | Summary | 711 |
| | Acknowledgments | 711 |
| | Pertinent Literature | 712 |
| | Section 16.3 | 712 |
| | Section 16.4 | 713 |
| | References | 714 |
| 17 | Multifrequency Electron Spin-Relaxation Times | 719 |
| | <i>Gareth R. Eaton and Sandra S. Eaton</i> | |
| 17.1 | Introduction and Scope of the Chapter | 719 |
| 17.2 | Spin-Spin Relaxation, T ₂ and T _m | 720 |
| 17.2.1 | T _m for Fremy's Salt in Glassy Solvents | 723 |
| 17.2.2 | Exchange-Narrowed Species and the 10/3 Effect | 724 |
| 17.2.3 | Conducting Systems | 725 |
| 17.2.4 | Metal Ions in Solution | 726 |
| 17.2.5 | Pb ³⁺ in Calcite | 726 |
| 17.3 | Spin-lattice Relaxation, T ₁ | 726 |
| 17.3.1 | Phonon Densities | 727 |
| 17.3.2 | Practical Interpretation of Relaxation Time Data as a Function of Temperature | 729 |

| | | |
|-----------|--|------------|
| 17.3.3 | Glasses versus Crystals | 729 |
| 17.3.4 | Spectral Diffusion and Cross-Relaxation | 731 |
| 17.3.5 | Effect of Pairs and Clusters | 732 |
| 17.3.6 | Magnetic Field Dependence of Relaxation | 732 |
| 17.3.6.1 | The Direct Process | 732 |
| 17.3.6.2 | The Raman Process | 734 |
| 17.3.6.3 | The Orbach Process | 734 |
| 17.3.6.4 | The Thermally Activated Process | 735 |
| 17.3.6.5 | Local Modes | 735 |
| 17.3.7 | Dependence of Relaxation on Magnetic Field Position in a CW-EPR Spectrum | 736 |
| 17.3.8 | Case Studies of Experimental Data | 737 |
| 17.3.8.1 | Nitroxyl Spin Labels | 737 |
| 17.3.8.2 | Semiquinones | 741 |
| 17.3.8.3 | Triarylmethyl (Trityl) Radicals | 742 |
| 17.3.8.4 | DPPH | 742 |
| 17.3.8.5 | Conducting Spin Systems | 742 |
| 17.3.8.6 | Metal ions in Fluid Solution | 743 |
| 17.3.8.7 | Relaxation at 2 mm Wavelength (150 GHz) | 746 |
| 17.3.9 | Fullerenes | 747 |
| 17.3.10 | Summary | 747 |
| | Acknowledgments | 748 |
| | Pertinent Literature | 748 |
| | References | 748 |
| 18 | EPR Imaging: Theory and Instrumentation | 755 |
| | <i>Rizwan Ahmad and Periannan Kuppusamy</i> | |
| 18.1 | Introduction | 755 |
| 18.2 | EPR Principle: Zeeman Effect | 756 |
| 18.2.1 | Hyperfine Splitting | 757 |
| 18.2.2 | Spin Relaxation | 759 |
| 18.2.3 | Comparison to NMR | 759 |
| 18.2.4 | EPR Probes | 759 |
| 18.3 | CW-EPR Imager | 760 |
| 18.3.1 | Magnets and Magnetic Field Control | 761 |
| 18.3.2 | Gradient Coil Assembly | 762 |
| 18.3.3 | RF Bridge | 764 |
| 18.3.4 | EPR Resonator | 765 |
| 18.3.5 | Signal Channel | 768 |
| 18.4 | Data Acquisition for CW-EPR and EPRI | 769 |
| 18.4.1 | Spectroscopy | 769 |
| 18.4.2 | Spatial EPRI | 770 |
| 18.4.3 | Spectral–Spatial EPRI | 772 |
| 18.5 | Important Imaging Parameters | 774 |

| | | |
|-----------|---|------------|
| 18.5.1 | Time Constant of Lock-In Amplifier | 774 |
| 18.5.2 | Modulation Amplitude | 775 |
| 18.5.3 | Gradient Strength | 775 |
| 18.6 | Image Reconstruction | 776 |
| 18.6.1 | Direct Methods | 777 |
| 18.6.1.1 | Filtered Backprojection (FBP) Method | 777 |
| 18.6.1.2 | Fourier-Based Reconstruction | 778 |
| 18.6.2 | Iterative Methods | 779 |
| 18.6.3 | Spectral–Spatial Reconstructions | 781 |
| 18.6.4 | Image Quality and Resolution | 782 |
| 18.7 | Other Data Collection Modalities | 783 |
| 18.7.1 | Pulsed-EPR | 783 |
| 18.7.2 | Single Point Imaging | 784 |
| 18.7.3 | Rapid Scan | 784 |
| 18.7.4 | Spinning Gradient | 784 |
| 18.8 | Constraints for Biological Applications | 785 |
| 18.9 | Special Imaging Applications | 786 |
| 18.9.1 | EPR Oximetry Mapping | 786 |
| 18.9.2 | Imaging Redox Metabolism in Tissues | 788 |
| 18.9.2.1 | Differential Distribution of Nitroxide Probes in Normal versus Tumor Tissue | 788 |
| 18.9.2.2 | Differential Metabolism of Nitroxide Probes in Normal versus Tumor Tissue | 789 |
| 18.10 | Scope and Limitations | 790 |
| | Acknowledgments | 791 |
| | Pertinent Literature | 791 |
| | References | 791 |
| 19 | Multifrequency EPR Microscopy: Experimental and Theoretical Aspects | 795 |
| | <i>Aharon Blank</i> | |
| 19.1 | General | 795 |
| 19.2 | Introduction | 795 |
| 19.2.1 | Definition | 795 |
| 19.2.2 | Historical Overview | 796 |
| 19.2.3 | “Induction Detection” versus Other Detection Methods | 797 |
| 19.3 | General Experimental Aspects of EPR Microscopy | 798 |
| 19.3.1 | CW-EPR Microscopy | 798 |
| 19.3.1.1 | System Configuration | 798 |
| 19.3.1.2 | Signal-to-Noise Ratio | 803 |
| 19.3.1.3 | Resolution | 805 |
| 19.3.2 | Pulsed-EPR Microscopy | 805 |
| 19.3.2.1 | System Configuration | 805 |
| 19.3.2.2 | SNR | 808 |

| | | |
|-----------|--|------------|
| 19.3.2.3 | Resolution | 810 |
| 19.4 | Specific Aspects of Multifrequency EPR Microscopy at Various Temperatures | 811 |
| 19.4.1 | SNR in a Multifrequency Context | 812 |
| 19.4.2 | Resolution in a Multifrequency Context | 814 |
| 19.5 | Illustrative Examples | 815 |
| 19.5.1 | Pulsed-EPR Microscopy of Solid Samples at Room Temperature | 816 |
| 19.5.2 | Pulsed-EPR Microscopy of Liquid Samples at Room Temperature | 816 |
| 19.5.3 | CW-EPR Microscopy of Solid and Liquid Samples at Room Temperature | 819 |
| 19.6 | Conclusions and Future Prospects | 821 |
| | Acknowledgments | 821 |
| | Pertinent Literature | 821 |
| | References | 822 |
| 20 | EPR Studies of Nanomaterials | 825 |
| | <i>Alex Smirnov</i> | |
| 20.1 | Introduction | 825 |
| 20.2 | EPR Studies of Magnetic Nanostructures | 827 |
| 20.3 | Characterization of Nanostructured Oxide Semiconductors for Photoactivated Catalysis and Solar Energy Conversion | 832 |
| 20.4 | Surface Radicals, Catalytic Activity, Cytotoxicity, and Radical-Scavenging Properties of Nanomaterials | 833 |
| 20.4.1 | Catalytic Activity | 833 |
| 20.4.2 | Cytotoxicity | 834 |
| 20.4.3 | Radical-Scavenging Properties | 835 |
| 20.5 | Spin-Labeling EPR Studies of Ligand-Protected Nanoparticles and Hybrid Nanostructures | 835 |
| 20.6 | Summary and Future Perspectives | 841 |
| | Acknowledgments | 842 |
| | Pertinent Literature | 842 |
| | References | 842 |
| 21 | Single-Molecule Magnets and Magnetic Quantum Tunneling | 845 |
| | <i>Sushil K. Misra</i> | |
| 21.1 | Introduction | 845 |
| 21.1.1 | Intramolecular Coupling | 846 |
| 21.1.2 | Examples of SMMs Reported in the Literature | 847 |
| 21.1.3 | Applications | 851 |
| 21.2 | Multifrequency EPR of SMMs: Magnetic Hysteresis and MQT | 852 |
| 21.2.1 | The Effective Spin Hamiltonian | 853 |
| 21.2.2 | Magnetic Quantum-Mechanical Tunneling (MQT) and MF-EPR | 854 |
| 21.2.3 | Zero-Field EPR with Variable Frequency | 854 |

| | | |
|-----------|---|-----|
| 21.2.4 | Low-Field (X-band) EPR | 854 |
| 21.2.5 | MF High-Frequency EPR | 855 |
| 21.2.5.1 | EPR Spectrometers with MF Cavity (40–350 and Extended Range 18–350 GHz), and up to 650 GHz Without a Cavity | 855 |
| 21.2.5.2 | Polycrystalline Powder EPR Spectrum | 855 |
| 21.2.5.3 | The Virtues of Single-Crystal Measurements | 855 |
| 21.2.5.4 | A Typical SMM Spectrum | 857 |
| 21.2.5.5 | EPR Linewidth Measurements: Effect of D-Strain, <i>g</i> -Strain, Dipolar and Exchange Interactions | 857 |
| 21.2.5.6 | Study of Intermolecular Exchange Interactions and Dipolar Interactions | 860 |
| 21.2.5.7 | EPR Spectra for Mn ₄ Family | 861 |
| 21.2.6 | Effect of Molecular Site Symmetry on Tunneling Phenomenon (MQT) as Revealed by EPR | 863 |
| 21.3 | Magnetic Quantum Tunneling (MQT): Pure and Thermally Assisted Tunneling | 867 |
| 21.3.1 | Relaxation of Magnetization for SMMs | 867 |
| 21.3.2 | Magnetic Hysteresis, Resonant Magnetization Tunneling in High-Spin Molecules and Thermally Assisted Resonant Tunneling Between Quantum States | 868 |
| 21.4 | Concluding Remarks | 872 |
| | Acknowledgments | 872 |
| | Pertinent Literature | 872 |
| | References | 872 |
| 22 | Multifrequency EPR on Photosynthetic Systems | 875 |
| | <i>Sushil K. Misra, Klaus Möbius, and Anton Savitsky</i> | |
| 22.1 | Introduction | 875 |
| 22.2 | Noxygenic Photosynthesis | 880 |
| 22.3 | Multifrequency EPR on Bacterial Photosynthetic Reaction Centers (RCs) | 882 |
| 22.3.1 | X-band EPR Experiments | 882 |
| 22.3.2 | 95-GHz EPR on Primary Donor Cations P ⁺ in Single-Crystal RCs | 883 |
| 22.3.3 | 360-GHz EPR on Primary Donor Cations P ⁺ in Mutant RCs | 884 |
| 22.3.4 | Results of <i>g</i> -tensor Computations of P ⁺ | 885 |
| 22.3.5 | 95-GHz EPR and ENDOR on the Acceptors Q _A [−] and Q _B [−] | 885 |
| 22.3.6 | 95-GHz ESE-Detected EPR on the Spin-correlated Radical Pair P ⁺ Q _A [−] | 892 |
| 22.3.7 | 95-GHz RIDME and PELDOR on the Spin-Correlated Radical Pair P ⁺ Q _A [−] | 893 |
| 22.3.8 | Multifrequency EPR on Primary Donor Triplet States in RCs | 895 |
| 22.4 | Oxygenic Photosynthesis | 897 |
| 22.4.1 | Multifrequency EPR on Doublet States in Photosystem I (PS I) | 897 |
| 22.4.2 | Multifrequency EPR on Doublet States in Photosystem II (PS II) | 900 |

| | | |
|-----------|--|------------|
| 22.5 | Concluding Remarks | 902 |
| | Acknowledgments | 904 |
| | Pertinent Literature | 904 |
| | References | 905 |
| 23 | Measurement of Superconducting Gaps | 913 |
| | <i>Sushil K. Misra</i> | |
| 23.1 | Introduction | 913 |
| 23.2 | The Superconducting Gap | 913 |
| 23.3 | Measurement of SCG | 914 |
| 23.4 | Concluding Remarks | 917 |
| | Acknowledgments | 918 |
| | References | 919 |
| 24 | Dynamic Nuclear Polarization (DNP) at High Magnetic Fields | 921 |
| | <i>Thomas Prisner and Mark J. Prandolini</i> | |
| 24.1 | Introduction | 921 |
| 24.2 | Historical Aspects (Metals, Solids and Liquids) at Lower Magnetic Fields | 922 |
| 24.3 | Theory | 924 |
| 24.3.1 | The Overhauser Effect (OE) | 924 |
| 24.3.2 | Two-Spin Cross-Polarization: Solid Effect (SE) | 930 |
| 24.3.3 | Many-Spin Cross-Polarization: Thermal Mixing (TM) | 931 |
| 24.3.4 | Three-Spin Cross-Polarization: Cross Effect (CE) | 933 |
| 24.3.5 | Beyond Classical DNP Methods: Coherent Polarization Transfer | 935 |
| 24.4 | Hardware (High-Frequency Microwave Equipment, SS-MAS DNP, HF-Liquid DNP, Dissolution DNP, Shuttle-DNP) | 936 |
| 24.4.1 | High-Frequency Microwave Sources | 936 |
| 24.4.2 | Transmission Lines | 937 |
| 24.4.3 | Spectrometer Types | 938 |
| 24.4.3.1 | Solid-State Magic Angle Spinning (MAS) DNP | 938 |
| 24.4.3.2 | Low-Temperature Dissolution Polarizer | 939 |
| 24.4.3.3 | <i>In-Situ</i> Temperature-Jump DNP (Laser Melting) | 940 |
| 24.4.3.4 | High-Field (HF) Liquid-DNP Spectrometers | 940 |
| 24.4.3.5 | Shuttle DNP | 941 |
| 24.5 | First Applications and Outlook | 942 |
| 24.5.1 | Application Areas of High-Field DNP | 942 |
| 24.5.2 | Outlook | 943 |
| | Acknowledgments | 943 |
| | Pertinent Literature | 943 |
| | References | 944 |
| 25 | Chemically Induced Electron and Nuclear Polarization | 947 |
| | <i>Lawrence J. Berliner and Elena Bagryanskaya</i> | |
| 25.1 | Introduction | 947 |

| | | |
|----------|--|-----|
| 25.2 | History of the CIDNP Phenomenon | 948 |
| 25.3 | The Radical Pair Mechanism | 948 |
| 25.3.1 | The Mechanism of Singlet–Triplet Conversion in RPs | 949 |
| 25.4 | Chemically Induced Dynamic Nuclear Polarization | 952 |
| 25.4.1 | The CIDNP Experiment | 955 |
| 25.4.2 | Time-Resolved CIDNP | 956 |
| 25.4.3 | Low Magnetic Field CIDNP | 958 |
| 25.4.4 | The Application of CIDNP to Biological Systems | 960 |
| 25.4.5 | Photo-CIDNP in the Study of Protein Folding | 961 |
| 25.4.6 | CIDNP Application to Study Primary Processes in the Bacterial Photosynthetic Center | 963 |
| 25.4.7 | CIDNP Applications to Electron Transfer in Peptide and Amino Acids | 966 |
| 25.5 | Chemically Induced Dynamic Electron Polarization | 967 |
| 25.5.1 | Triplet Mechanism of CIDEП | 967 |
| 25.5.2 | Radical-Pair Mechanism of CIDEП | 969 |
| 25.5.2.1 | CIDEП Due to S–T ₀ Transitions | 969 |
| 25.5.3 | CIDEП Due to S–T ₋ and S–T ₊ Transitions | 970 |
| 25.5.4 | CIDEП Due to the Radical-Triplet Pair Mechanism | 971 |
| 25.5.5 | CIDEП Due to the SCRP Mechanism | 972 |
| 25.5.6 | CIDEП Kinetics | 974 |
| 25.5.6.1 | Modified Bloch Equations | 974 |
| 25.5.7 | Time-Resolved EPR Spectroscopy | 974 |
| 25.5.8 | CIDEП Applications | 976 |
| 25.5.9 | Applications of CIDEП to Biological Systems | 980 |
| 25.5.10 | Applications of CIDEП to Study Photochemical Reaction Centers | 981 |
| 25.5.11 | RTPM CIDEП in Spin-Labeled Peptides | 981 |
| 25.5.12 | Applications of CIDEП to Studies of Biological Function: Protein Dynamics and Protein–Surface Interactions | 982 |
| 25.5.13 | CIDEП Study of Amino Acid Photooxidation | 983 |
| 25.6 | Conclusion | 984 |
| | Pertinent Literature | 986 |
| | References | 988 |

Part Four Future Perspectives 993

| | | |
|-----------|--|------|
| 26 | Future Perspectives | 995 |
| | <i>Sushil K. Misra</i> | |
| 26.1 | Spectroscopic Techniques Currently Available in EPR | 995 |
| 26.1.1 | Future Perspectives in EPR Instrumentation | 997 |
| 26.1.2 | Desirable Advancements in EPR Instrumentation | 998 |
| 26.2 | Cutting-Edge Topics | 999 |
| 26.2.1 | Topics Related to the Theoretical Interpretation of EPR Data | 1002 |

| | | |
|------|-------------------------------|------|
| 26.3 | Desirable Applications of EPR | 1003 |
| 26.4 | Future of EPR | 1003 |
| | Acknowledgments | 1004 |

| | | |
|--------------------|---|-------------|
| Appendix A1 | Fundamental Constants and Conversion Factors used in EPR | 1005 |
| Index | | 1009 |